Theory and Simulation of Vibrational Coupling in Deuterated Proteins: Toward a New Structural Probe?†

Johanna Becker, Franz Becher, Oliver Hucke, Andreas Labahn, and Thorsten Koslowski*

Institut für Physikalische Chemie, Universität Freiburg, Albertstrasse 23a, D-79104 Freiburg im Breisgau, Germany

Received: April 9, 2003; In Final Form: July 25, 2003

In this work, we present a theoretical and numerical analysis of the vibrational coupling of two deuterated structural elements in proteins. Depending on the presence and magnitude of coupling between these elements, typically deuterium atoms connected to α carbons, characteristic level splittings of vibrational eigenstates are predicted, which are observable around 2100 cm^{-1} in a broad and transparent spectral window. This approach is illustrated and substantiated by the application of classical force fields to the simulation of the vibrational density of states of the crambin protein. We discuss the possibility to use this effect to obtain structural information about proteins and suggest experiments to verify our theoretical approach.

1. Introduction

In recent years, isotope substitution has become an important technique in biochemical applications of infrared spectroscopy. Deuteration of nonexchangeable positions has turned out to be a particularly useful tool because it shifts selected C−H bond stretching modes into the spectral region around 2100 cm^{-1}, which lies in a broad transparent window between C═O (1700 cm^{-1}) and CH_2 (2850 cm^{-1}) vibrations. In turn, the detection and the interpretation of the IR signal are simplified considerably. The thus-shifted modes are interpreted as localized and essentially reduced to single C−D vibrations.[1,2] To our knowledge, this was first demonstrated for a protein by Chin et al., who have presented a study of the C−D vibrations of labeled horse heart cytochrome *c*.[2] In that work, the methyl group of Met80 was completely deuterated, and the position and line width were used as a probe of the redox state of the Fe ion and its coordination by cyanide or nitric oxide. The same authors have used this label to correlate line positions and widths to the redox activity in mutants of the same protein.[3] In addition, deuteration in infrared spectroscopy has been used to obtain information about the conformation and dynamics of molecules, including the conformational analysis of alkylamino chains[4] and nucleosides,[5] protein−lipid interactions,[6−9] and the conformation of membrane proteins.[10] For biomolecules, deuteration can be achieved according to the following strategies: the introduction of isotope-labeled precursors into a metabolic pathway,[2] de novo protein synthesis,[10,11] cell-free protein synthesis with a modified suppressor tRNA,[12] or a eukaryotic cell-free translational system.[13]

Most of the previous studies were performed either with a single deuterated amino acid or under conditions where a significant fraction of the macromolecule has been deuterated. Very recently, Torres and Arkin[10] have used two consecutive alanine residues with deuterated methyl groups to study the helix tilt and rotational orientation of the transmembrane segment of a protein from influenza A virus by attenuated total reflection infrared dichroism. In this work, we present a simple theory of vibrational coupling between two deuterated structural entities, which gives rise to a particular spectroscopic pattern once they are in close spatial contact and thus coupled by short-range interactions. This model leads to a simple fingerprint of coupling, which is illustrated and substantiated by the computation of the vibrational density of states using classical force fields. The results are discussed, and experiments are suggested to verify or falsify the theoretical and numerical findings presented here.

2. Two-Oscillator Model

In the following, the numerical findings presented below are rationalized and quantified within a simple two-oscillator model.[1] As will become evident from the numerical simulations, the modes under consideration are spatially localized and energetically distinct from both the remaining bending and stretching modes. Consequently, they are decoupled, and in terms of the Hessian, first-order degenerate perturbation theory applies.

We consider the C−D stretching modes of two deuterated structural elements, which are characterized by frequencies ω_1 and ω_2 in the hypothetical absence of coupling. This case is referred to as DD in an obvious notation. In Cartesian coordinates, the potential energy V representing two oscillators with the reduced masses m_1 and m_2, displacements from equilibrium by u_1 and u_2 and a coupling parameter D' is given by

$$V = \frac{1}{2}m_1\omega_1^2u_1^2 + \frac{1}{2}m_2\omega_2^2u_2^2 - D'u_1u_2 \qquad (2.1)$$

which leads to the coupled Newtonian equations of motion

$$m_1\ddot{u}_1 + m_1\omega_1^2u_1 - D'u_2 = 0 \quad \text{and}$$
$$m_2\ddot{u}_2 + m_2\omega_2^2u_2 - D'u_1 = 0 \qquad (2.2)$$

In the absence of coupling, that is, $D' = 0$, these equations are reduced to those of simple harmonic oscillators, $m_i\ddot{u}_i =$

† Dedicated to Prof. Peter Gräber on the occcassion of his 60th birthday.

* Corresponding author. Fax: +49-761-203-6189. E-mail: Thorsten.Koslowski@physchem.uni-freiburg.de.

10.1021/jp034944x CCC: $25.00
Published on Web 10/29/2003

$-m_i\omega_i^2 u_i$, $i = 1$ and 2. The coupled equations can be solved using displacements that are periodic in time, $u_i = A_i \cos(\omega t + \phi)$ with frequency ω, amplitudes A_i, and phase shift ϕ, following eqs 2.7.6 and 2.7.7 of ref 1. Using mass-weighted coordinates (eq 2.7.14 of ref 1), we arrive at the secular equation

$$|\mathbf{F} - \lambda\mathbf{E}| = \begin{vmatrix} \omega_1^2 - \lambda & -D \\ -D & \omega_2^2 - \lambda \end{vmatrix} = 0 \qquad (2.3)$$

with $D = D'/\sqrt{m_1 m_2}$, Hessian matrix $\mathbf{F}$, and unit matrix $\mathbf{E}$. As solutions of the eigenvalue problem, we obtain two frequencies $\omega = \sqrt{\lambda}$, which are a function of ω_1, ω_2, and D. We note that eq 2.3 is identical to eq 2.7.15 of ref 1 with $\omega_1^2 = (f_1 + f_{12})/m_1$, $\omega_2^2 = (f_2 + f_{12})/m_2$, and $D = f_{12}/\sqrt{m_1 m_2}$, where the right-hand sides are written using the notation of that reference with force constants f_1, f_2, and f_{12} and reduced masses m_1 and m_2. We obtain the eigenvalues

$$\lambda_{1,\mathrm{DD}} = \frac{\omega_1^2 + \omega_2^2}{2} - \frac{1}{2}\sqrt{(\omega_1^2 - \omega_2^2)^2 + 4D^2} \qquad (2.4a)$$

$$\lambda_{2,\mathrm{DD}} = \frac{\omega_1^2 + \omega_2^2}{2} + \frac{1}{2}\sqrt{(\omega_1^2 - \omega_2^2)^2 + 4D^2} \qquad (2.4b)$$

which we denote as $\lambda_{1,\mathrm{DD}} = \omega_\mathrm{A}^2$ and $\lambda_{2,\mathrm{DD}} = \omega_\mathrm{B}^2$. Between a symmetric and an antisymmetric combination mode, a level splitting of

$$\Delta\lambda_{\mathrm{DD}} = \sqrt{(\omega_1^2 - \omega_2^2)^2 + 4D^2} = \omega_\mathrm{A}^2 - \omega_\mathrm{B}^2 \qquad (2.5)$$

can be computed. The frequencies ω_1 and ω_2 and the coupling matrix element D depend on the reduced masses of the vibrational entities. If deuterium is replaced by hydrogen in one of the entities, a case referred to as HD or DH, these quantities will be denoted as $\tilde{\omega}_1$, $\tilde{\omega}_2$, and $\tilde{D}$. The frequencies within the pairs $\tilde{\omega}_1^2 - \omega_2^2$ and $\omega_1^2 - \tilde{\omega}_2^2$ now differ considerably (by roughly 10^3 cm^{-1} in terms of wavenumbers) and are also considerably larger than the square root of the coupling matrix element, $\tilde{D}^{1/2}$. Therefore, the square root in eqs 2.4a and 2.4b can be expanded; for the DH problem, the Taylor expansion up to the first two terms reads

$$\sqrt{(\omega_1^2 - \tilde{\omega}_2^2)^2 + 4\tilde{D}^2} \simeq \omega_1^2 - \tilde{\omega}_2^2 + \frac{2\tilde{D}^2}{\omega_1^2 - \tilde{\omega}_2^2} \qquad (2.6)$$

A lower eigenvalue of

$$\lambda_{1,\mathrm{DH}} = \omega_1^2 - \frac{\tilde{D}^2}{\tilde{\omega}_2^2 - \omega_1^2} = \omega_\mathrm{C}^2 \qquad (2.7)$$

emerges for the DH problem. For its HD counterpart,

$$\lambda_{1,\mathrm{HD}} = \omega_2^2 - \frac{\tilde{D}^2}{\tilde{\omega}_1^2 - \omega_2^2} = \omega_\mathrm{D}^2 \qquad (2.8)$$

holds. The corrections with reference to the unperturbed frequencies ω_1 and ω_2 are small and amount to less than 10^{-2} cm^{-1} for all examples presented in this work. From a physical perspective, the reduction of the reduced mass upon hydration effectively decouples the deuterium and the hydrogen stretching modes. As a consequence, the difference in the lower eigenvalues between the DH and the HD problem is within a high degree of accuracy given by

$$\Delta\lambda_{\mathrm{DH,HD}} = \omega_2^2 - \omega_1^2 \qquad (2.9)$$

(cf. eqs 2.7 and 2.8). The coupling strength between the two vibrating entities, $\Delta\omega$, can thus be obtained from four observable quantities, the deuterium vibrational frequencies $\omega_\mathrm{A} = \lambda_{1,\mathrm{DD}}^{1/2} = 2\pi c\tilde{\nu}_\mathrm{A}$, $\omega_\mathrm{B} = \lambda_{2,\mathrm{DD}}^{1/2} = 2\pi c\tilde{\nu}_\mathrm{B}$, $\omega_\mathrm{C} = \lambda_{1,\mathrm{HD}}^{1/2} = 2\pi c\tilde{\nu}_\mathrm{C}$, and $\omega_\mathrm{D} = \lambda_{1,\mathrm{DH}}^{1/2} = 2\pi c\tilde{\nu}_\mathrm{D}$, determined from three experiments (DD, HD, and DH substitution). We finally arrive at a simple expression for the quantity of interest,

$$D = \Delta\omega^2 = \frac{1}{2}\{(\omega_\mathrm{A}^2 - \omega_\mathrm{B}^2)^2 - (\omega_\mathrm{C}^2 - \omega_\mathrm{D}^2)^2\}^{1/2} \qquad (2.10)$$

From our point of view, the simple two-oscillator model presented here can also be applied to interpret the coupling of more complex vibrations, for example, those originating from deutered methyl or methylene groups. For CH_2-groups, symmetric and antisymmetric modes are separated by 70 cm^{-1}, and CH_3 symmetric and antisymmetric modes are split by 83 cm^{-1} (deuterated: 43 cm^{-1}); these numbers hold for phospholipids.[14] For a quantitative analysis, it is highly desirable to use the entire set of four ($CH_2\cdots H_2C$) or six ($CH_3\cdots H_3C$) bond stretching vibrations as a basis for a perturbative vibrational analysis. In the absence of special symmetries, this analysis has, however, to be performed numerically, including the computation of the intensities via the resulting normal modes. On the other hand, because the through-space couplings between two CH_2 or CH_3 groups are small compared to the symmetric−antisymmetric splittings, two pairs of split levels will arise, which are dominated by either symmetric−symmetric or antisymmetric−antisymmetric contributions. Thus, either symmetric *or* antisymmetric vibrations enter the simple two-oscillator vibrational Hamiltonian rather than the CH stretching modes. Consequently, the level splittings can still be interpreted in terms of the coupling effect described above.

3. Simulation

To test the hypothesis formulated above within a more advanced model appropriate to the description of proteins on a microscopic level, we have performed the computation of vibrational spectra for partly deuterated biopolymers. For these computations, we have selected crambin from *Crambe abyssinica*, of which a high-resolution X-ray structure is available.[15−18] In addition, NMR studies of a mutant[19] not only allow an assessment of the structure in solution but also give an impression of the flexibility of the protein structure, an issue that will become important once the validity of the harmonic model used here is discussed. Furthermore, crambin has been the subject of computer simulations due to its relatively small size and structural integrity. The macromolecule has been described as a compact globular protein with a molecular weight of ∼5 kDa[15] with a total of 46 amino acids. Its shape resembles the Greek letter Γ with a stem consisting of an antiparallel pair of helices, a cross-arm of two antiparallel β-strands, an irregular strand, and a β-turn.[16] According to Llinás et al.,[20] it exhibits an exceptional degree of rigidity, a feature that can be rationalized by the occupation of the inner bend of the backbone by side chains and by the presence of numerous salt bridges, hydrogen bonds, and other contacts.[16] In addition, three disulfide bridges stabilize the structure.

As a basis of our computations, we have applied the X-ray structure from the work of Hendrickson and Teeter.[15−17] Hydrogen atoms were added by using a routine of the WHATIF

package,[21] which is based on an algorithm described by Vriend.[22] Three different force fields—AMBER,[23] CHARMM,[24] and MM3[25]—have been used for the microscopic description of the protein based on classical mechanics. Throughout this work, Ponder's TINKER suite of programs[26] has been utilized to optimize the geometries and compute the matrix elements of the Hessian. We have also used the parametrized force fields referenced above as implemented in the TINKER package. For a numerical study of protein vibrations, a tight relaxation is imperative; its quality can be assessed by the final gradient norms, which were always smaller than 10^{-6} kcal mol^{-1} Å^{-1}, and the moduli of the six smallest eigenvalues of the Hessian matrix, which did not exceed 10^{-6} cm^{-2}. Here, theory requires six vanishing eigenvalues, which can be identified as the three translational and rotational degrees of freedom of the molecule.[1] Within all calculations, water molecules have been omitted. Although interesting aggregates of H_2O have been detected on the amphipathic surface of the protein,[17] none of these molecules is in close contact with the amino acids that finally turn out to participate in vibrational coupling.

The calculation of vibrational eigenvalues (giving rise to the frequencies) and the corresponding eigenvectors (representing the atomic displacements or amplitudes of the corresponding normal modes) requires the computation of the Hessian matrix, that is, the matrix of mixed second derivatives of the potential energy with respect to all coordinates under consideration. With the use of Cartesian coordinates u_{ia} and u_{jb}, the matrix elements read[1,27]

$$D_{iajb} = (m_i m_j)^{-1/2} \frac{\partial^2 V}{\partial u_{ia} \partial u_{jb}} \tag{3.1}$$

with atomic indices i and j and Cartesian components a and $b \in \{x, y, z\}$. The dependence of the matrix elements on the reduced atomic masses is obvious, and elementary arguments stemming from the theory of matrices lead to a frequency shift to the red once an atom is replaced by an isotope larger in mass. Diagonalization of the $3N \times 3N$ Hessian matrix that represents the interactions between N atoms leads to eigenvalues $\omega_\alpha^2 = \omega_1^2, ..., \omega_{3N}^2$ and the corresponding normal modes

$$\vec{q}_\alpha = \sum_{i=1}^{N} \sum_{a=1}^{3} c_{ia\alpha} u_{ia} \vec{e}_{ia} \tag{3.2}$$

To identify those vibrational couplings relevant to structural patterns of the proteins, we have proceeded as follows. In the spectral region of hydrogen-bond stretching (2800−3300 cm^{-1}) the modes of the undeuterated biopolymer have been visually inspected for those vibrations that exhibit an amplitude on at least two amino acids. To select a couple of residues, two conditions should be fulfilled: a close proximity between the residues in space but a position far apart in the primary sequence of the protein. Of these, the most promising pairs are Cys4−Cys32 and Pro5−Tyr44, where in either case the coupling originates from hydrogen atoms bound to C_α atoms, to which we will refer as H_α. We note that vibrational coupling along a sulfur bridge is nontrivial because it has not been observed for the Cys3−Cys40 and the Cys16−Cys26 pairs because of the large interhydrogen distances, ranging from 5.27 to 5.90 Å, regardless of the force field. For the thus-selected pairs of amino acids, the following isotope substitutions have been performed: (1) H_α by D_α for the first amino acid only, which corresponds to the DH case described above; (2) H_α by D_α, restricted to the second amino acid, the HD case; (3) H_α by D_α for both amino acids, the DD pattern formulated above.

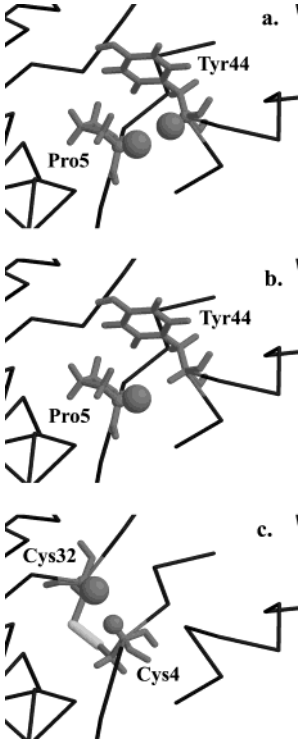

Figure 1. Representation of vibrational eigenstates as computed using the CHARMM force field: (a) Pro5−Tyr44, DD (symmetrically coupled oscillators); (b) Pro5−Tyr44, DH (decoupled oscillators); (c) Cys4−Cys32, DD (asymmetric coupling). The radii of the spheres are proportional to the local amplitudes via the local norm eq 3.3. Black indicates the protein backbone, dark gray indicates the coupling amino acids, and light gray indicates the disulfide bridge (in Figure 1c only).

For practical reasons, namely, the availability of the corresponding amino acids, we have also studied the HD, DH, and DD substitution patterns for fully deuterated amino acids. Examples of vibrations of selectively deuterated crambin as computed using the CHARMM force field are presented in Figure 1 for the Pro5−Tyr44 pair (DD, Figure 1a) and the Cys4−Cys32 pair (DD, Figure 1c). Here, the radii of the spheres represent, within an arbitrary global norm, the amplitude of the vibrations on atom i via the local norm

$$n_{i\alpha} = \sqrt{{c_{ix\alpha}}^2 + {c_{iy\alpha}}^2 + {c_{iz\alpha}}^2}. \tag{3.3}$$

The first vibration is symmetric concerning the local norms, and a counterpart with reversed $n_{i\alpha}$ and $n_{j\alpha}$, which is not shown here, exists. The last vibration is asymmetric in this respect, and it is separated from its counterpart by only 0.3 cm^{-1}. As evident from these figures, the vibrations are localized in space, but exhibit contributions on amino acids far apart in the sequence of protein building blocks. In Figure 1b, only the hydrogen atom connected to the Pro5 C_α atom has been replaced by deuterium (DH case), and further localization and decoupling are obvious. All vibrations studied are also presented in Tables 1 and 2, where the wavenumbers of the decoupled vibrational levels, $\tilde{\nu}_C$ and $\tilde{\nu}_D$, and their coupled counterparts, $\tilde{\nu}_A$ and $\tilde{\nu}_B$, are listed. Whenever the difference $|\tilde{\nu}_A - \tilde{\nu}_B|$ exceeds the splitting in the absence of coupling, $|\tilde{\nu}_C - \tilde{\nu}_D|$, by more than the resolution obtainable within an experiment, the effect should be detectable. Because classical force fields only provide a limited accuracy in predicting vibrational energy levels,[28] a perfect agreement between the AMBER, CHARMM, and MM3 results cannot be expected. The same statement holds for a quantitative comparison to experiments, whereas we believe that the spectroscopic

TABLE 1: Computed Crambin Vibrational Modes for the Pro5 and Tyr44 Contact, Wavenumbers in the Absence of Coupling ($\tilde{\nu}_C$, $\tilde{\nu}_D$) and in Its Presence ($\tilde{\nu}_A$, $\tilde{\nu}_B$), and Coupling Matrix Element *D* Computed from eq 2.10 Using ω_A, ω_B, ω_C, and ω_D as Obtained from the Simulated Spectra

	coupled		decoupled			
force field	$\tilde{\nu}_A$, cm^{-1}	$\tilde{\nu}_B$, cm^{-1}	$\tilde{\nu}_C$, cm^{-1}	$\tilde{\nu}_D$, cm^{-1}	D, cm^{-2}	figure
AMBER	2195.9	2201.2	2200.4	2196.7	8 054	
CHARMM	2161.2	2167.7	2164.3	2164.6	14 099	1a,b; 2a
MM3	2170.9	2185.6	2179.9	2176.5	31 150	

TABLE 2: Computed Crambin Vibrational Modes for the Cys4−Cys32 Contact, Wavenumbers in the Absence of Coupling ($\tilde{\nu}_C$, $\tilde{\nu}_D$) and in its Presence ($\tilde{\nu}_A$, $\tilde{\nu}_B$), and Coupling Matrix Element *D* Computed from eq 2.10 Using ω_A, ω_B, ω_C, and ω_D as Obtained from the Simulated Spectra

	coupled		decoupled			
force field	$\tilde{\nu}_A$, cm^{-1}	$\tilde{\nu}_B$, cm^{-1}	$\tilde{\nu}_C$, cm^{-1}	$\tilde{\nu}_D$, cm^{-1}	D, cm^{-2}	figure
AMBER	2197.3	2200.6	2197.8	2200.0	5267	
CHARMM	2162.6	2167.0	2164.0	2165.6	8957	1c; 2b,c
MM3	2163.6	2194.2	2163.7	2194.0		

patterns discussed here do not depend on the minute details of the underlying interactions. For the Pro5−Tyr44 pair, the AMBER results are likely to lie in the range of the experimental resolution, whereas differences in the level distances upon decoupling, $\Delta\tilde{\nu} = |\tilde{\nu}_A - \tilde{\nu}_B| - |\tilde{\nu}_C - \tilde{\nu}_D| = 6.2$ cm^{-1} for the CHARMM and 11.3 cm^{-1} for the MM3 force field are more than encouraging (Table 1). For the Cys4−Cys32 coupling, only the CHARMM force field predicts an observable effect (2.8 cm^{-1}), whereas MM3 exhibits a vanishing coupling (Table 2).

The corresponding vibrational densities of states based upon computations using the CHARMM force field are displayed in Figure 2. The lines have been broadened by a Gaussian function with a root mean square (RMS) deviation of 2 cm^{-1}, corresponding to a line width of 5 cm^{-1}. The decoupled HD and DH spectra are drawn as dots, whereas the coupled DD cases are presented as full lines. In Figure 2a, the Pro5−Tyr44 HD and DH lines are almost degenerate; they split significantly upon coupling. In Figure 2b, the Cys4−Cys32 HD and DH lines can be distinguished, and a considerable additional broadening can be observed upon coupling. In these two cases, the DD spectrum is notably distinct from the sum of the HD and the DH spectra, which for experiments set a clear fingerprint for the detection of through-space vibrational coupling. A qualitative analysis can be performed using eq 2.10. Vibrational coupling persists upon complete deuteration of the participating amino acids; the example of Cys4−Cys32 is presented in Figure 2c. Here, the same pattern as in Figure 2b can be observed around 2165 cm^{-1}, whereas the spectrum below 2158 cm^{-1} can be rationalized as the sum of the HD and DH spectra, indicating the absence of vibrational coupling between the participating deuterium atoms.

The distances associated with the vibrational couplings are listed in Table 3. As expected, both the deuterium−deuterium distances and the $C_\alpha-C_\alpha$ spacings are small and close to the sum of the two van der Waals radii ($\sigma_H = 2.2$ Å[29]). To address the question of the correlation between the local geometry and the strength of the coupling, we have analyzed the difference between the level splitting in the presence of coupling and in its absence, $\Delta\tilde{\nu} = |\tilde{\nu}_A - \tilde{\nu}_B| - |\tilde{\nu}_C - \tilde{\nu}_D|$, as a function of the inverse interdeuterium distance, r_{DD}. This analysis has been performed for a total of 21 pairs (seven contacts with three force fields each), of which nine give rise to an effect with $\Delta\tilde{\nu} > 0.1$ cm^{-1}. The results are displayed in Figure 3. In addition to the Cys4−Cys32 and Pro4−Tyr44 pairs, a through-space vibrational coupling was observed for Thr2−Ile34, Arg17−Thr21, and

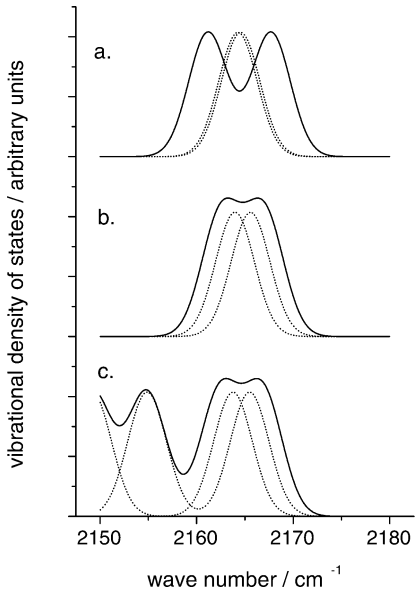

Figure 2. Simulated vibrational density of states for (a) Pro5−Tyr44, (b) Cys4−Cys32 (C_αD), and (c) Cys4−Cys32 (full deuteration). Full line represents coupling (DD vibrations); dots represent decoupling (DH and HD vibrations). All computations were performed using the CHARMM force field.

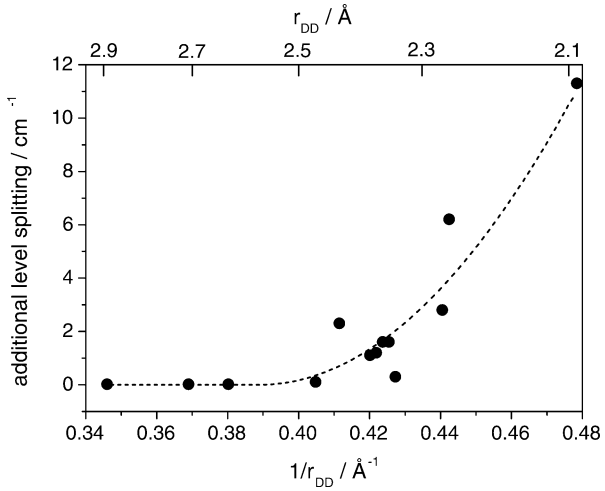

Figure 3. Additional level splitting upon coupling, $\Delta\tilde{\nu} = |\tilde{\nu}_A - \tilde{\nu}_B| - |\tilde{\nu}_C - \tilde{\nu}_D|$, as a function of the inverse interdeuterium distance.

TABLE 3: Important Interatomic Distances in Å and ϕ_{CDCD} Orientational Angles in deg as Obtained from an Analysis of the Experimental Structure (Carbon Atoms[16,18]), the Addition of Hydrogen Atoms to this Structure Using the WHATIF Package, and Geometries Optimized Using the AMBER, CHARMM, and MM3 Force Fields, as Referenced in the Text

		experiment/			
amino acids	parameter	WHATIF	AMBER	CHARMM	MM3
Cys4, Cys32	$H_\alpha-H_\alpha$	2.31	2.38	2.28	2.34
	$C_\alpha-C_\alpha$	4.09	4.16	4.11	4.19
	ϕ_{CDCD}		127	129	122
Pro5, Tyr44	$H_\alpha-H_\alpha$	2.29	2.36	2.26	2.09
	$C_\alpha-C_\alpha$	4.17	4.29	4.29	4.21
	ϕ_{CDCD}		152	144	152

Asn12−Val15. In view of the nonbonding interactions entering the force fields, it is tempting to speculate about a strong negative exponential or inverse power law dependence of the additional splitting upon the interdeuterium distance. From our perspective, however, the amount and quality of the data only allow a statement along the line that an effect of ∼3 cm^{-1} should

be detectable experimentally at spacings on the order of $r_{DD} = 2.3-2.4$ Å or smaller and that the decay of the coupling is stronger than an inverse proportional dependence. The latter finding is less evident from the dependence of the coupling effect at small distances but from its vanishing at ~2.6 Å. In addition, we have evidence for an increasing additional level splitting with an increasing C−D−C−D orientational angle in the interval between 120° and 150°. This holds for contacts with $r_{DD} < 2.6$ Å, and the effect is weak and difficult to separate from the aforementioned dependence on r_{DD}. We note that the splitting is also a function of the spacing between the unperturbed lines, which may differ from one amino acid contact to the other.

To describe an infrared spectrum, the vibrational density of states alone is not sufficient; it has to be supplemented by information on the transition dipole moments. Because C−H and C−D bond stretching vibrations in proteins are, however, experimentally detectable, we do not expect a serious effect beyond a possible asymmetric distribution of the intensities that characterize a pair of lines: a symmetric combination will decrease in intensity; an asymmetric one will enhance the IR signal.

We are aware of the fact that decoupling upon deuteration of a single amino acid also occurs within the spectral region of C−H bond stretching (to which one may refer, using the notation described above, as DH−HD−HH). Therefore, FTIR (Fourier transform infrared) difference spectroscopy (for a review, see ref 30, for example) may provide a tool to detect the weak changes in intensity upon decoupling. As an advantage of this scheme in contrast to the DH−HD−DD approach, only two instead of three deuteration experiments have to be performed. In addition, it opens the possibility to scan systematically for amino acid contacts by the consecutive deuteration of amino acids. In a similar fashion, ^{13}C isotope substitutions may become useful to study vibrational coupling within the amide I region.[31]

As the largest obstacle in observing the splitting patterns predicted here, we consider inhomogeneous line broadening due to the dynamics of larger protein segments, which may in general lead to a strongly fluctuating distance between the amino acids under consideration. For the crambin contacts studied here, however, general structural considerations,[20] X-ray temperature factors,[15−17] NMR studies,[19] and molecular dynamics simulations[32] indicate a high degree of structural conservation, which holds in particular for the protein backbone, to which the coupling D_α atoms are bound.

4. Conclusions

In this work, we have presented a simplified theory of the vibrational coupling between two fully or partly deuterated amino acids in a close spatial neighborhood. When the amino acids couple, a vibrational level splitting extending the spectral distance between the corresponding lines of the singly deuterated amino acids is predicted. These findings have been illustrated by computations of the vibrational density of states of Cys4−Cys32 and Pro5−Tyr44 couplings in crambin using classical force fields. These calculations further substantiate the theoretical findings.

From our point of view, the selective deuteration of two amino acids can provide important structural information in terms of the corresponding spatial contact between atoms located on the residues. This technique probes distance-dependent interactions rather than the separation within the sequence of amino acids. As a consequence, the detection of couplings between amino acids far apart within this sequence would introduce an additional constraint to a three-dimensional model of the protein structure and thus provide significant structural information on a level comparable to NOESY experiments. This information may turn out to be particularly helpful in the study of membrane proteins.[11] In the protein studied here, only a small number of contacts gives rise to the coupling patterns described above. Consequently, the absence of these patterns does not necessarily imply a large spatial separation between the two amino acids under consideration.

As an experimental test to verify or falsify our approach, we suggest infrared spectroscopy of the deuterated crambin amino acids, for example Cys4, Pro5, Cys23, and Tyr44, following the scheme presented in this work.

Acknowledgment. It is a pleasure to thank P. Gräber and A. Blumen for fruitful discussions and helpful comments. We gratefully acknowledge the use of the TINKER program package.[26]

References and Notes

(1) Wilson, E. B., Jr.; Decius, J. C.; Cross, P. C. *Molecular Vibrations*; Dover Publications: New York, 1955.

(2) Chin, J. K.; Jimenez, R.; Romesberg, F. E. *J. Am. Chem. Soc.* **2001**, *123*, 2426−2427.

(3) Chin, J. K.; Jimenez, R.; Romesberg, F. E. *J. Am. Chem. Soc.* **2002**, *124*, 1846−1847.

(4) Ohno, K.; Nomura, S.; Yoshida, H.; Matsuura, H. *Spectrochim. Acta A* **1999**, *55*, 2231−2246.

(5) Grajcar, L.; Baron, M. H.; Becouran, S.; Czernecki, S.; Valery, J. M.; Reiss, C. *Spectrochim. Acta A* **1994**, *50*, 1015−1022.

(6) Dluhy, R. A.; Mendelsohn, R.; Casal, H. L.; Mantsch, H. H. *Biochemistry* **1983**, *22*, 1170−1177.

(7) Pastrana, B.; Mautone, A. J.; Mendelsohn, R. *Biochemistry* **1991**, *30*, 10058−10064.

(8) Echabe, I.; Requero, M. A.; Goni, F. M.; Arrondo, J. L. R.; Alonso, A. *Eur. J. Biochem.* **1995**, *231*, 199−203.

(9) Fraile, M. V.; Lopez-Rodriguez, G.; Gallego-Nicasio, J.; Carmona, P. *Biopolymers* **2000**, *57*, 11−18.

(10) Torres, J.; Arkin, I. T. *Biophys. J.* **2002**, *82*, 1068−1075.

(11) Torres, J.; Kukol, A.; Arkin, I. T. *Biophys. J.* **2000**, *79*, 3139−3143.

(12) Sonar, S.; Lee, C. P.; Coleman, M.; Patel, N., Liu, X.; Marti, T.; Khorana, G. H.; RajBhandary, U. L.; Rothschild, K. J. *Nat. Struct. Biol.* **1994**, *1*, 512−517.

(13) Bergo, V.; Mamaev, S.; Olejnik, J.; Rothschild, K. J. *Biophys. J.* **2003**, *84*, 960−966.

(14) Winter, R.; Noll, F. *Methoden der Biophysikalischen Chemie*; Teubner: Stuttgart, Germany, 1989; p 359.

(15) Teeter, M. M.; Hendrickson, W. A. *J. Mol. Biol.* **1979**, *127*, 219−223.

(16) Hendrickson, W. A.; Teeter, M. M. *Nature* **1981**, *290*, 107−113.

(17) Teeter, M. M. *Proc. Natl. Acad. Sci. U.S.A.* **1984**, *81*, 6014−6018.

(18) Brookhaven protein data database (PDB) entry 1CRN.

(19) Bonvin, A. M. J. J.; Rullmann, J. A. C.; Lamerichs, R. M. J. N.; Boelens, R.; Kaptein, R. *Proteins* **1993**, *15*, 385−400.

(20) LLinás, M.; De Marco, A.; Lecomte, J. T. J. *Biochemistry* **1980**, *19*, 1140−1145.

(21) Vriend, G. *J. Mol. Graphics* **1990**, *8*, 52−56.

(22) Hooft, R. W. W.; Sander, C.; Vriend, G. *Proteins* **1996**, *26*, 363−376.

(23) (a) Pearlman, D. A.; Case, D. A.; Caldwell, J. W.; Ross, W. S.; Cheatham, T. E.; DeBolt, S.; Ferguson, D.; Seibel, G.; Kollman, P. *Comput. Phys. Commun.* **1995**, *91*, 1−41. (b) Cornell, W. D.; Cieplak, P.; Bayly, C. I.; Gould, I. R.; Merz, K. M.; Ferguson, D. M.; Spellmeyer, D. C.; Fox, T.; Caldwell, J. W.; Kollman, P. A. *J. Am. Chem. Soc.* **1995**, *117*, 5179−5197. (c) Kollman, P.; Dixon, R.; Cornell; Fox, T.; Chipot, C.; Pohorille, A. In *Computer Simulation of Biomolecular Systems*; van Gunsteren, W. F., Weiner, P. K., Wilkinson, A. J., Eds.; Kluwer Academic Publishers: Dordrecht, The Netherlands; 1997; Vol. 3, pp 3−96. (d) Moyna, G.; Williams, H. J.; Nachman, J.; Scott, A. I. *Biopolymers* **1999**, *49*, 403−413.

(24) (a) Brooks, B. R.; Bruccoleri, R. E.; Olafson, B. D.; States, D. J.; Swaminathan, S.; Karplus, M. *J. Comput. Chem.* **1983**, *4*, 187−217. (b) MacKerell, A. D., Jr.; Bashford, D.; Bellott, M.; Dunbrack, R. L., Jr.; Evanseck, J. D.; Field, M. J.; Fischer, S.; Gao, J.; Guo, H.; Ha, S.; Joseph-McCarthy, D.; Kuchnir, L.; Kuczera, K.; Lau, F. T. K.; Mattos, C.; Michnick, S.; Ngo, T.; Nguyen, D. T.; Prodhom, B.; Reiher, W. E., III; Roux, B.; Schlenkrich, M.; Smith, J. C.; Stote, R.; Straub, J.; Watanabe,

M.; Wiórkiewicz-Kuczera, J.; Yin, D.; Karplus, M. *J. Phys. Chem. B* **1998**, *102*, 3586−3616. (c) Foloppe, N.; MacKerell, A. D. *J. Comput. Chem.* **2000**, *21*, 86−104.

(25) (a) Allinger, N. L.; Yuh, Y. H.; Lii, J.-H. *J. Am. Chem. Soc.* **1989**, *111*, 8551−8566. (b) Lii, J.-H.; Allinger, N. L. *J. Am. Chem. Soc.* **1989**, *111*, 8566−8575. (c) Lii, J.-H.; Allinger, N. L. *J. Am. Chem. Soc.* **1989**, *111*, 8576−8582. (d) Lii, J.-H.; Allinger, N. L. *J. Phys. Org. Chem.* **1994**, *7*, 591−609. (e) Lii, J.-H.; Allinger, N. L. *J. Comput. Chem.* **1994**, *19*, 1001−1016.

(26) (a) Pappu, R. V.; Hart, R. K.; Ponder, J. W. *J. Phys. Chem. B* **1998**, *102*, 9725−9742. (b) Dudek, M. J.; Ramnarayan, K.; Ponder, J. W. *J. Comput. Chem.* **1998**, *19*, 548−573. (c) Kong, Y.; Ponder, J. W. *J. Chem. Phys.* **1997**, *107*, 481−492. (d) Ponder, J. W.; Richards, F. M. *J. Comput. Chem.* **1987**, *8*, 1016−1024.

(27) Madelung, O. *Festkörpertheorie I*; Heidelberger Taschenbücher; Springer-Verlag: Heidelberg, Germany, 1972.

(28) Schubach, J. B. Infrarotspektroskopie komplexer Systeme. Ph.D. Thesis, Albert-Ludwigs Universität, Freiburg, Germany, 2000.

(29) Pauling, L. *General Chemistry*, 3rd ed.; W. H. Freeman and Company: San Francisco, CA, 1970.

(30) Arrondo, J. L. R.; Muga, A.; Castresana, J.; Goni, F. M. *Prog. Biophys. Mol. Biol.* **1993**, *59*, 23−56.

(31) Moritz, R.; Fabian, H.; Hahn, U.; Diem, M.; Naumann, D. *J. Am. Chem. Soc.* **2002**, *124*, 6259−6264.

(32) Caves, L. S. D.; Evanseck, J. D.; Karplus, M. *Protein Sci.* **1998**, *7*, 649−666.